Agricultural Water Management 209 (2018) 188–196

Contents lists available at ScienceDirect

Agricultural Water Management

journal homepage: www.elsevier.com/locate/agwat

Simulating kernel number under different water regimes using the Water-Flowering Model in hybrid maize seed production

Jintao Wang, Shaozhong Kang*, Xiaotao Zhang, Taisheng Du, Ling Tong, Risheng Ding, Sien Li

Center for Agricultural Water Research in China, China Agricultural University, Beijing, 100083, China

ARTICLE INFO

Keywords:
Flowering characteristics
Water deficit
Relative evapotranspiration
Maize pollen density
Seed-set capacity

ABSTRACT

Flowering Model, can accurately simulate the kernel number of maize based on the flowering characteristics and is very suitable for hybrid maize seed production where the number of pollen grain is always the main strain for kernel formation. However, it isn't suitable for the water deficit condition. Therefore, the Water-Flowering Model was built by incorporating the seed-set capacity of female plant into Flowering Model and simulating the effect of water deficit on flowering characteristics in the form of water production function. The experiment conducted at Shiyanghe Experimental Station of China Agricultural University in 2014 and 2015 was used to calibrate and validate the Water-Flowering Model, respectively. The regression coefficient (b), determination coefficient (R^2), relative root mean square error (RRMSE), Nash and Sutcliff modelling efficiency (EF), average relative error (ARE) and concordance index d of Willmott between the measured data and simulated results of 2015 was 0.78, 0.78, 0.2787, 0.29, 0.2501 and 0.84, respectively. To some extent, the model can be used to simulate kernel number in hybrid maize seed production under different water regimes in this area. But the key parameter, pollen density threshold (PD_{min}), is heavily influenced by meteorological factors. Therefore, PD_{min} should be related to meteorological factors instead of using an average value during the flowering stage to accurately simulate kernel number using Water-Flowering Model.

1. Introduction

In hybrid maize seed production, the pollen supply is always limited by the less ratio of male inbreds (Fonseca et al., 2004), and sometimes the synchrony between pollen shed and silking is disturbed without altering crop growth rate by the unsuitable plant date of male and female inbreds. Most models for simulating maize yield mainly concentrate on fertilization and kernel formation. But they can't take the effect of pollen density and synchrony in floral development into account (Fonseca et al., 2004; Lizaso et al., 2003). Flowering Model (Lizaso et al., 2003) can simulate kernel number of maize based on flowering characteristics and is very suitable for hybrid maize seed production. However, Flowering Model assumes that all the fertilized ovaries are able to develop into kernels. Therefore, the Flowering Model has mainly been applied in fields with hybrid maize seed production under no stress conditions (Fonseca et al., 2004; Lizaso et al., 2003). However, if water deficit happens, some of the fertilized ovaries will abort and can't develop into kernels (Alqudah et al., 2011), therefore the original Flowering Model isn't suitable for this circumstance.

The seed-set capacity (SC) of the female plant indicates the ability of pollinated female flowers to allow for pollen tube germination, development, and connection with the ovary carpel as well as indicating the ability of fertilized ovaries to set kernels (Alqudah et al., 2011; Bassetti and Westgate, 1993; Kiesselbach, 1980; Westgate and Boyer, 1986b). Wang et al. (2017) reported that the SC decreased under water deficit at the vegetative and flowering stages because of the low water potential of silk and the reduction of assimilate supply. Therefore, the SC needs to be incorporated into the Flowering Model in order to simulate kernel numbers under different water regimes.

As flowering characteristics were changing with water conditions (Wang et al., 2017), whenever the water condition changes the flowering characteristics need to be measured all over again to accurately simulate kernel number of maize (Lizaso et al., 2003). The laborious measurement of flowering characteristics makes the Flowering Model inconvenient to be applied under different water conditions. It is, therefore, necessary to determine the effect of water deficits on the flowering characteristics to simulate kernel number accurately under different water regimes using the Flowering Model with a unified set of parameters.

The effect of water deficit on flowering characteristics of maize has been studied by many researches. For example, water deficit at the vegetative stage delayed pollen shed time and decreased pollen shed

* Corresponding author.
E-mail address: kangsz@cau.edu.cn (S. Kang).

https://doi.org/10.1016/j.agwat.2018.07.014
Received 12 January 2018; Received in revised form 5 July 2018; Accepted 17 July 2018
Available online 01 August 2018

Table 1
Irrigation treatments at establishment, vegetative, flowering, yield-formation and ripening stages of maize inbred for hybrid seed production in 2014 and 2015.

Year	Treatment[a]	Establishment	Vegetative	Flowering	Yield-formation	Ripening
2014	V2F2	0	100[b]	100	100	100
	V2F1	0	100	50	100	100
	V2F0	0	100	0	100	100
	V1F2	0	50	100	100	100
	V1F1	0	50	50	100	100
	V0F2	0	0	100	100	100
	V0F0	0	0	0	100	100
2015	V2F2	0	100	100	100	100
	V2F1	0	100	50	100	100
	V2F0	0	100	0	100	100
	V1F2	0	50	100	100	100
	V1F1	0	50	50	100	100
	V1F0	0	50	0	100	100
	V0F2	0	0	100	100	100
	V0F1	0	0	50	100	100
	V0F0	0	0	0	100	100

[a] F, flowering stage; V, vegetative stage. Numbers 0, 1, and 2 indicate no irrigation (Stage 0), 50% of full irrigation (Stage 1), and full irrigation (Stage 2), respectively. In the control treatment (V2F2), the irrigation lower limit was maintained at 70 ± 2% of the field water capacity, and the upper limit was maintained at the field water capacity during the whole season.
[b] Irrigation amounts: 100, full irrigation; 50, 50% of full irrigation amount; 0, no irrigation.

rate of maize (Wang et al., 2017). And water deficit at both vegetative and flowering stages decreased pollen number (Alqudah et al., 2011; Westgate and Boyer, 1986a), delayed silking time (Dudley et al., 1971; Schoper et al., 1986), and decreased silking rate, the number of exposed silks and SC of ear (Fuad-Hassan et al., 2008; Horner and Palmer, 1995; Westgate and Boyer, 1986b; Wilson and Allison, 1978). But, these studies about the responses of flowering characteristics to water deficit are all qualitative, and to our knowledge there is no quantitative study.

Crop water production functions originally related crop yield with evapotranspiration at different growth stages to quantitatively describe the effects of water deficit at each growth stage on the crop yield (Blank, 1975; Jensen, 1968; Kang et al., 2017; Minhas et al., 1974; Stewart et al., 1975). Çakir (2004) treated the quantitative effects on yield of water deficit in vegetative and reproductive stages of hybrid maize using crop water production function, but not in relation to the flowering characteristics. Recently, the forms of crop water production functions were used to quantitatively describe the effects of water deficit at different growth stages on the fruit qualities of tomato (Chen et al., 2014). Therefore, based on the responses of flowering characteristics to water deficit at the vegetative and flowering stages in our previous study (Wang et al., 2017), we can develop the water production function for flowering characteristics of maize inbreds for hybrid seed production to get the water sensitivity indexes and predict flowering characteristics by evapotranspiration.

Thus, the objective of this study is to develop, calibrate and validate a Water-Flowering Model, based on the Flowering Model and the effect of water deficit on flowering characteristics, to simulate kernel number of maize by the relative evapotranspiration.

2. Materials and methods

2.1. Field experiment

The experiment was conducted at Shiyanghe Experimental Station of China Agricultural University, located in Wuwei City, Gansu Province of northwest China (37°52′ N, 102°50′ E, altitude 1581 m) in 2014 and 2015. The female inbreds were planted on 15 Apr. 2014 and 16 Apr. 2015. Six days later, the first batch of male inbreds (Male1) was planted and another six days later the second batch of male inbreds (Male2) was planted. The planting pattern was 5 female rows alternated with 1 male row. The row spacing was 40 cm, and the plant spacing was 25 cm for the female inbreds and 30 cm for the male inbreds. The two batches of male inbreds were planted in the same rows, alternating four plants of Male1 with four plants of Male2. Before pollen shedding, the female inbreds were detasseled. The male inbreds were cut at the early yield-formation stage. Kernel was harvested on 20 Sept. 2014 and 15 Sept. 2015. Before planting, basal fertilizer of 136 kg N ha^{-1}, 225 kg P_2O_5 ha^{-1}, and 300 kg K_2O ha^{-1} was spreaded over the fields. Top dressing of 364 kg N ha^{-1} was applied on 5 June 2014 and 9 June 2015 (Wang et al., 2017). The weeds were removed manually and the pest was controlled by pyridaben.

There were 7 irrigation treatments in 2014 and 9 irrigation treatments in 2015 during the vegetative (V, from the sixth leaf stage to the tasseling stage) and flowering (F, including tasseling, pollen shedding, and silking) stages. There were three irrigation levels, i.e. full irrigation (labelled as 2), 50% of full irrigation (labelled as 1) and no irrigation (labelled as 0), at both stages V and F. The lower irrigation limit of the full irrigated treatment (V2F2) was set at 70 ± 2% FC, and upper irrigation limit was set at FC during the whole season. Except for the vegetative and flowering stages, irrigation amount of all the treatments was maintained the same as V2F2 during the rest of season. All treatments were irrigated at the same time as V2F2 (Wang et al., 2017). Soil water content was measured by TRIME-PICO (TDR, IMKO, Germany). Crop actual evapotranspiration was calculated by water balance method using the average soil moisture changes in the 0–100 cm soil layer (Kang et al., 2000). As groundwater table is deeper than 25 m, the contribution of groundwater to the soil water was negligible in the study area. No surface runoff and deep drainage occurred during irrigation. The irrigation amount and evapotranspiration of vegetative and flowering stages for each treatment were presented in Table 1. A brief description to the measurements of the input flowering characteristics was presented in Table 2. For the details of the measurement of flowering characteristics and kernel number, please refer to Wang et al. (2017).

2.2. Description of Water-Flowering Model

(1) The original Flowering Model
Flowering Model can simulate kernel number of maize based on the flowering characteristics. For the details of Flowering Model, see Lizaso et al. (2003). The brief description is as follows:

$$KN_t = \frac{ks_t \times CSN_t \times E_{APt}}{Fplants} \quad (1)$$

where KN_t is the kernel number per ear forming on the t *th* day of

Table 2
The input flowering characteristics and a brief description to their measurements.

Flowering Progress	Flowering Characteristics	Brief Description of Measurements
Silking dynamics of population	T_f Eq. (5)	The percentage of plants with silks emerging on the apical ear (Silking: silks longer than 1 cm emerging from the surrounding husk) was recorded every other day.
	k_f Eq. (5)	
Dynamics of silk exsertion per ear	SN_X Eq. (6)	Every other day, a sample of emerged silk was taken from the selected female inbreds. The ear was re-bagged immediately to prevent pollination. The silk pieces were counted.
	k_e Eq. (6)	
	SC Eq. (7)	The pollination of the selected plants was prevented by covering the ears with bags. On the fourth or fifth day after silking, a sample of emerged silk was taken from the selected female inbreds and the silk pieces were counted. The remaining silks on the ear were hand-pollinated with sufficient pollen immediately after sampling and the ear was immediately re-bagged. The kernels on the ear pollinated by hand were counted at harvest time and SC was defined as the ratio of kernel number to the number of hand-pollinated silks.
	TPD Eq. (3)	The number of pollen grains per unit area was measured daily by passive pollen traps. TPD is the sum of pollen number per unit area during flowering stage.
Pollen shedding dynamics of population	$k_{jStartshed}$ Eq. (4)	The percentage of Malej plants that had started to shed pollen was recorded at each of three pollen shed stages (Startshed, when plants had started to shed pollen: anthers exerted on the main tassel branch only; Maxshed, at or past maximum pollen shed: anthers exerted on main and side tassel branches; and Endshed, plants had completed pollen shed: no new anthers exerted) every other day.
	$T_{jStartshed}$ Eq. (4)	
	$k_{jMaxshed}$ Eq. (4)	
	$T_{jMaxshed}$ Eq. (4)	
	$k_{jEndshed}$ Eq. (4)	
	$T_{jEndshed}$ Eq. (4)	

the year; ks_t is the percentage of exposed silks that pollinated on the t th day of the year; CSN_t is the accumulative number of exposed silks available for pollination on the t th day of the year; E_{APt} is the efficiency of kernel set considering the asynchrony within ear on the t th day of the year, which is controlled by the total number of exposed silks per ear and the accumulative kernel number per ear formed before the t th day of the year; *Fplants* is the number of female plants (plants ha^{-1}); t is the day of the year. The final kernel number per ear is the sum of the kernels per ear forming on each day during the flowering stage.

$$ks_t = 0.96 \times \frac{PD_t}{PD_{\min}} \quad 0 < PD_t \le PD_{\min}, \text{ and}$$
$$ks_t = 0.96 \quad PD_t > PD_{\min} \tag{2}$$

where PD_t is the pollen number per square centimeter at the ear level of female plant on the t th day of the year, i.e. pollen density (grains cm^{-2} d^{-1}) of male plants on the t th day of the year, which is the sum of pollen density of each batch of male plants on the t th day of the year; PD_{min} = 100 grains cm^{-2} d^{-1} is the pollen density threshold.

$$PD_{jt} = \frac{R_{indjt}}{100} \times \frac{Mplants_j}{Mplants} \times \frac{TPD}{sheddays_j} \tag{3}$$

where PD_{jt} is the pollen density of the j th batch of male parent (Malej) on the t th day of the year; R_{indtj} is the percentage of the Malej population in the average pollen shed state on the t th day of the year (%); $sheddays_j$ is the days that the average pollen shed state of an individual Malej plant last; $Mplants_j$ is the number of Malej plant (plants ha^{-1}); *TPD* is the total pollen density during the flowering stage (grains cm^{-2}).

R_{indtj} and $sheddays_j$ can be derived from pollen shed dynamics of male population which were described as sigmoid curves in the Flowering Model:

$$R_{jgt} = \frac{1}{1 + e^{-k_{jg} \times (t - T_{jg})}} \tag{4}$$

where R_{jgt} is the accumulative percentage of the Malej population which have reached the Startshed, Maxshed, Endshed stage (%), g represents pollen shed stage i.e. Startshed, Maxshed and Endshed. k_{jg} is the Startshed, Maxshed and Endshed rate of Malej population; T_{jg} is the day of Malej population reaching the Startshed, Maxshed and Endshed stage (day of year).

The accumulative number of exposed silks available for pollination on the t th day of the year (CSN_t) can be derived from the silking dynamic of female population and an individual ear, the percentage of exposed silks that pollinated from the *t-5* to t th day of the year (ks_{t-5} to ks_t) and the proportion of female plants. The silking dynamic of female population was described as a sigmoid curve and the silking dynamic of an individual ear was described as a monomolecular model in the Flowering Model:

$$R_{ft} = \frac{1}{1 + e^{-k_f \times (t - T_f)}} \tag{5}$$

where R_{ft} is the accumulated percentage of female population with exposed silks to the t th day of the year; k_f is the silking rate of female population; T_f is the silking time of female population (day of year).

$$SN_T = SN_X \times (1 - e^{-k_e \times T}) \tag{6}$$

where SN_T is the accumulated number of exposed silks to the T th day after the first silk exposed for an individual ear; SN_X is the total number of exposed silks per ear; k_e is the silking rate of an individual ear.

(2) Flowering Model revising

To simulate kernel number of maize under different water regimes, the seed-set capacity (SC) of the female plant needs to be incorporated into the Flowering Model. Therefore Eq. (1) should be changed as follows:

$$KN_t = \frac{SC \times ks_t \times CSN_t \times E_{APt}}{Fplants} \tag{7}$$

(3) Simulating the effect of water deficit on flowering characteristics

The input flowering characteristics in Flowering Model are shown in Table 2. Wang et al. (2017) found that water deficit at the vegetative and flowering stages decreased k_f, SN_X, k_e, SC and TPD, and increased T_f. Water deficit after the flowering stage had no influence on the flowering characteristics because the process of flowering had ended. Thus, the prediction model of k_f, T_f, SN_X, k_e, SC and TPD was based on the relative evapotranspiration at the vegetative and flowering stages of maize for seed production.

Four water production function model forms, i.e. Jensen model, Minhas model, Blank model and Stewart model, were compared to simulate the effect of water deficit at the vegetative and flowering stages on flowering characteristics and the best one was choosed as the

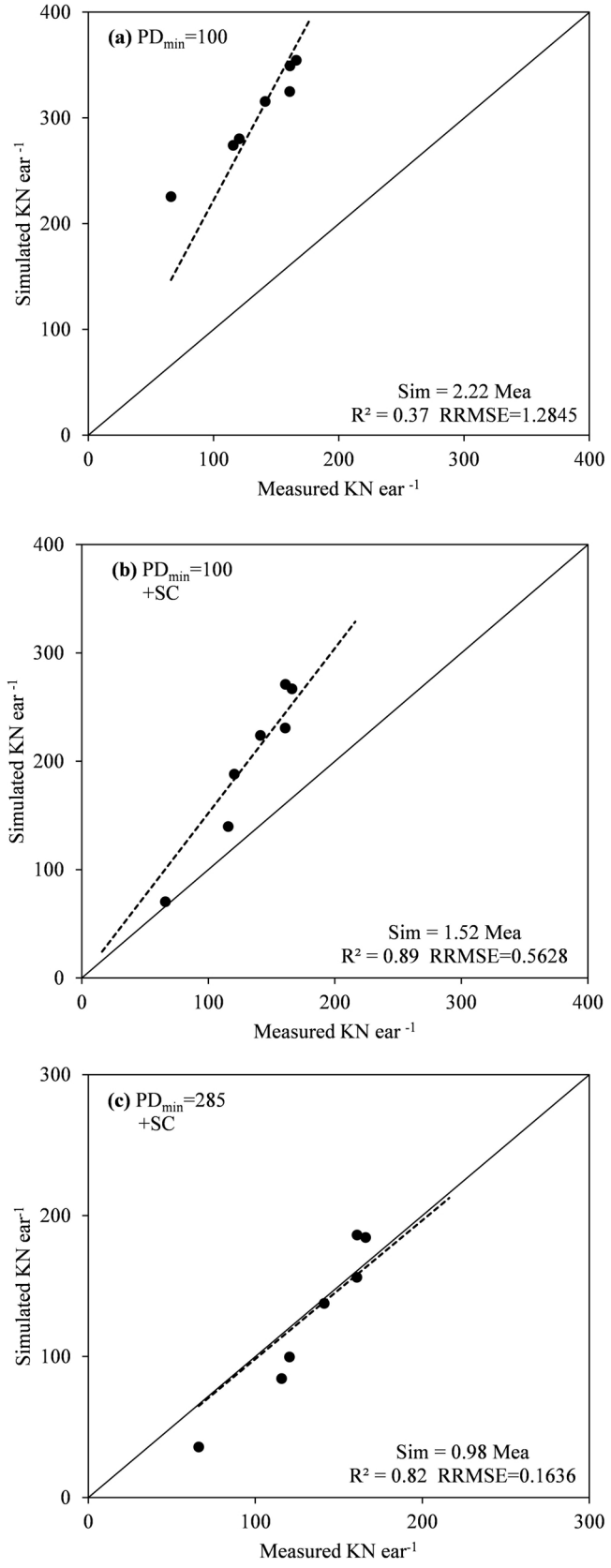

Fig. 1. Relationships between the measured kernel number (Mea) of 2014 and the simulated data (Sim) under different water conditions. (a) with the original Flowering Model; (b) with the revised Flowering Model; (c) the pollen density threshold (PD_{min}) was calibrated as 285 grains cm^{-2} d^{-1} in the revised Flowering Model based on the experimental data from 2014. R^2, the coefficient of determination; RRMSE, the relative root mean square error.

component of the Water-Flowering Model:

Jensen

$$\frac{F_a}{F_m} = \prod_{i=1}^{n} \left(\frac{ET_{ai}}{ET_{mi}}\right)^{\lambda_i} \tag{8}$$

Minhas

$$\frac{F_a}{F_m} = \prod_{i=1}^{n} \left(1 - \left(1 - \frac{ET_{ai}}{ET_{mi}}\right)^2\right)^{\delta_i} \tag{9}$$

Blank

$$\frac{F_a}{F_m} = \sum_{i=1}^{n} A_i \left(\frac{ET_{ai}}{ET_{mi}}\right) \tag{10}$$

Stewart

$$\frac{F_a}{F_m} = 1 - \sum_{i=1}^{n} B_i \left(1 - \frac{ET_{ai}}{ET_{mi}}\right) \tag{11}$$

where F_a is k_f、T_f、SN_X、k_e、SC and TPD in each treatment; F_m is k_f、T_f、SN_X、k_e、SC and TPD under full irrigation; ET_{ai} is the evapotranspiration at each growth stage of different treatments; ET_{mi} is the evapotranspiration at each growth stage of full irrigation treatment; λ_i, δ_i, A_i and B_i are the water deficit sensitivity index of k_f、T_f、SN_X、k_e、SC and TPD at each growth stage. i indicates the vegetative and flowering stage. $n = 2$ is the number of growth stages.

Wang et al. (2017) found that water deficit at the vegetative stage decreased Startshed, Maxshed and Endshed rate (k_{jg}, i.e. $k_{1Startshed}$, $k_{1Maxshed}$, $k_{1Endshed}$, $k_{2Startshed}$, $k_{2Maxshed}$, $k_{2Endshed}$), and delayed Startshed, Maxshed and Endshed time (T_{jg}, i.e. $T_{1Startshed}$, $T_{1Maxshed}$, $T_{1Endshed}$, $T_{2Startshed}$, $T_{2Maxshed}$, $T_{2Endshed}$) of the two batches of male population. Water deficit at the flowering stage had no influence on k_{jg} and T_{jg}. Thus, the prediction model of k_{jg} and T_{jg} was based on the relative evapotranspiration of the vegetative stage:

$$\frac{F_{jga}}{F_{jgm}} = \beta \frac{ET_{Va}}{ET_{Vm}} + \gamma \tag{12}$$

where F_{jga} (j is the male batch; g is the pollen shed stage) is k_{jg} and T_{jg} of each treatment; F_{jgm} is k_{jg} and T_{jg} under full irrigation treatment; ET_{Va} is evapotranspiration at the vegetative stage of each treatment; ET_{Vm} is evapotranspiration at the vegetative stage under full irrigation treatment; β is the water deficit sensitivity index of k_{jg} and T_{jg} at the vegetative stage, and γ is the interception.

2.3. Calibration and validation

Parameters of the Water-Flowering Model were calibrated by the 7 sets of field experiment data of 2014, and the 9 sets of field experiment data of 2015 was used to validate the model. The regression coefficient (b), determination coefficient (R^2), relative root mean square error (RRMSE), Nash and Sutcliff modelling efficiency (EF), average relative error (ARE) and concordance index d of Willmott between the measured data and simulated results were calculated to evaluate the performance of the Water-Flowering Model (Coucheney et al., 2015; Yang et al., 2014):

$$b = \frac{\sum_{i=1}^{n} M_i S_i}{\sum_{i=1}^{n} M_i^2} \tag{13}$$

$$R^2 = \left[\frac{\sum_{i=1}^{n} (S_i - \overline{S})(M_i - \overline{M})}{\sqrt{\sum_{i=1}^{n} (S_i - \overline{S})^2 \sum_{i=1}^{n} (M_i - \overline{M})^2}}\right]^2 \tag{14}$$

$$RRMSE = \frac{1}{\overline{M}} \sqrt{\frac{1}{n} \sum_{i=1}^{n} (S_i - M_i)^2} \tag{15}$$

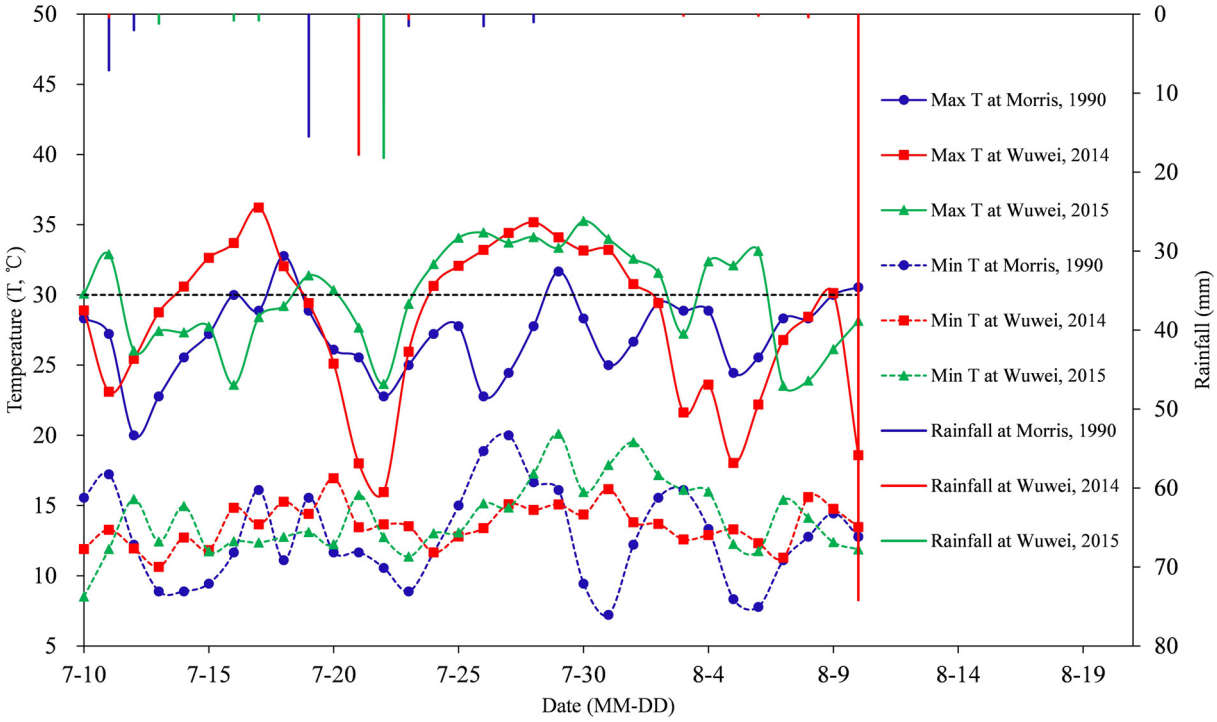

Fig. 2. The meteorological conditions at Morris, Minnesota in 1990 (data from http://w2.weather.gov/climate/xmacis.php?wfo=mpx) and at Wuwei, Gnasu in 2014 and 2015.

Table 3
Water sensitivity indexes of k_f, T_f, k_e, SN_X, SC and TPD at the vegetative and flowering stages for different models calibrated by 7 irrigation treatments of 2014. R^2, the coefficient of determination; RRMSE, the relative root mean square error. k_f, the silking rate of the female population; T_f, the silking time of the female population; k_e, the silking rate of an individual ear; SN_X, the total number of exposed silks per ear; SC, the seed-set capacity of the female plant; TPD, the total pollen density.

Flowering Characteristics	Models	Water sensitive index (λ/δ/A/B)		R^2	*RRMSE*
		Vegetative stage	Flowering stage		
k_f	Jensen	0.5092	0.2643	0.94	0.0587
	Minhas	1.2047	0.8530	0.88	0.0864
	Blank	0.5888	0.4096	0.99	0.0657
	Stewart	0.5916	0.2396	0.93	0.0582
T_f	Jensen	−0.0161	−0.0161	0.96	0.0014
	Minhas	−0.0389	−0.0477	0.94	0.0023
	Blank	−0.0223	−0.0206	0.93	0.0015
	Stewart	−0.0220	−0.0205	0.96	0.0015
k_e	Jensen	0.1653	0.1473	0.79	0.0411
	Minhas	0.3761	0.3757	0.72	0.0516
	Blank	0.3246	0.7220	0.98	0.1188
	Stewart	0.2173	0.1379	0.80	0.0390
SN_X	Jensen	0.1204	0.2812	0.88	0.0238
	Minhas	0.2700	0.4476	0.70	0.0325
	Blank	0.3127	0.7529	0.99	0.1127
	Stewart	0.1627	0.1628	0.89	0.0223
SC	Jensen	0.5499	1.0856	0.97	0.0511
	Minhas	1.2974	3.1341	0.95	0.0948
	Blank	0.5509	0.4050	0.99	0.0937
	Stewart	0.6514	0.7278	0.97	0.0476
TPD	Jensen	0.3462	0.1916	0.84	0.0713
	Minhas	0.8331	0.5873	0.79	0.0829
	Blank	0.4614	0.5578	0.99	0.0994
	Stewart	0.4165	0.1998	0.82	0.0711

Table 4
Water sensitivity indexes (β) of Startshed, Maxshed and Endshed rate and time of the two batches of male population calibrated by 7 irrigation treatments of 2014. R^2, the coefficient of determination; RRMSE, the relative root mean square error.

Flowering Characteristics	*β*	γ	R^2	*RRMSE*
$k_{1Startshed}$	0.6123	0.3787	0.96	0.0280
$T_{1Startshed}$	−0.0285	1.0284	0.95	0.0013
$k_{1Maxshed}$	0.6260	0.3764	0.88	0.0504
$T_{1Maxshed}$	−0.0266	1.0265	0.93	0.0014
$k_{1Endshed}$	0.4364	0.5551	0.85	0.0396
$T_{1Endshed}$	−0.0203	1.0197	0.94	0.0010
$k_{2Startshed}$	0.3850	0.6257	0.80	0.0407
$T_{2Startshed}$	−0.0167	1.0163	0.74	0.0019
$k_{2Maxshed}$	0.4666	0.5541	0.95	0.0215
$T_{2Maxshed}$	−0.0174	1.0174	0.83	0.0016
$k_{2Endshed}$	0.2383	0.7588	0.81	0.0238
$T_{2Endshed}$	−0.0092	1.0084	0.57	0.0015

$$EF = 1 - \frac{\sum_{i=1}^{n}(S_i - M_i)^2}{\sum_{i=1}^{n}(M_i - \overline{M})^2} \quad (16)$$

$$ARE = \frac{\frac{1}{n}\sum_{i=1}^{n}|S_i - M_i|}{\overline{M}} \quad (17)$$

$$d = 1 - \frac{\sum_{i=1}^{n}(S_i - M_i)^2}{\sum_{i=1}^{n}(|S_i - \overline{M}| + |M_i - \overline{S}|)^2} \quad (18)$$

where S_i and M_i are the simulated and measured values, respectively; $\overline{S}$ and $\overline{M}$ are the averages of the simulated and measured values, respectively; n is the number of measurements.

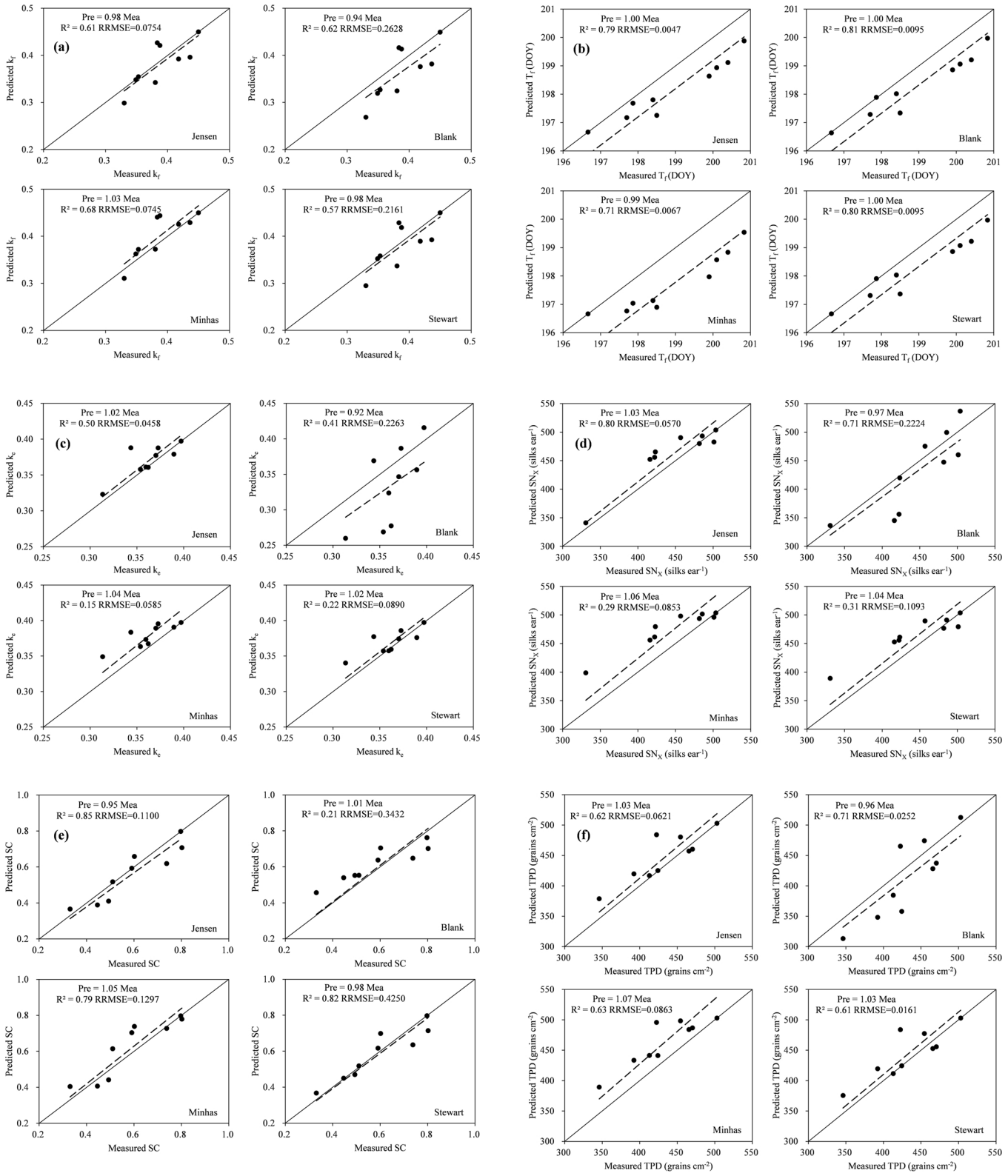

Fig. 3. Comparison between the measured flowering characteristics (Mea) of 2015 and the predicted (Pre) value by different models with the parameters calibrated by 7 irrigation treatments of 2014. (a) k_f, the silking rate of the female population; (b) T_f, the silking time of the female population; (c) k_e, the silking rate of an individual ear; (d) SN_X, the total number of exposed silks per ear; (e) SC, the seed-set capacity of the female plant; (f) TPD, the total pollen density. R^2, the coefficient of determination; RRMSE, the relative root mean square error.

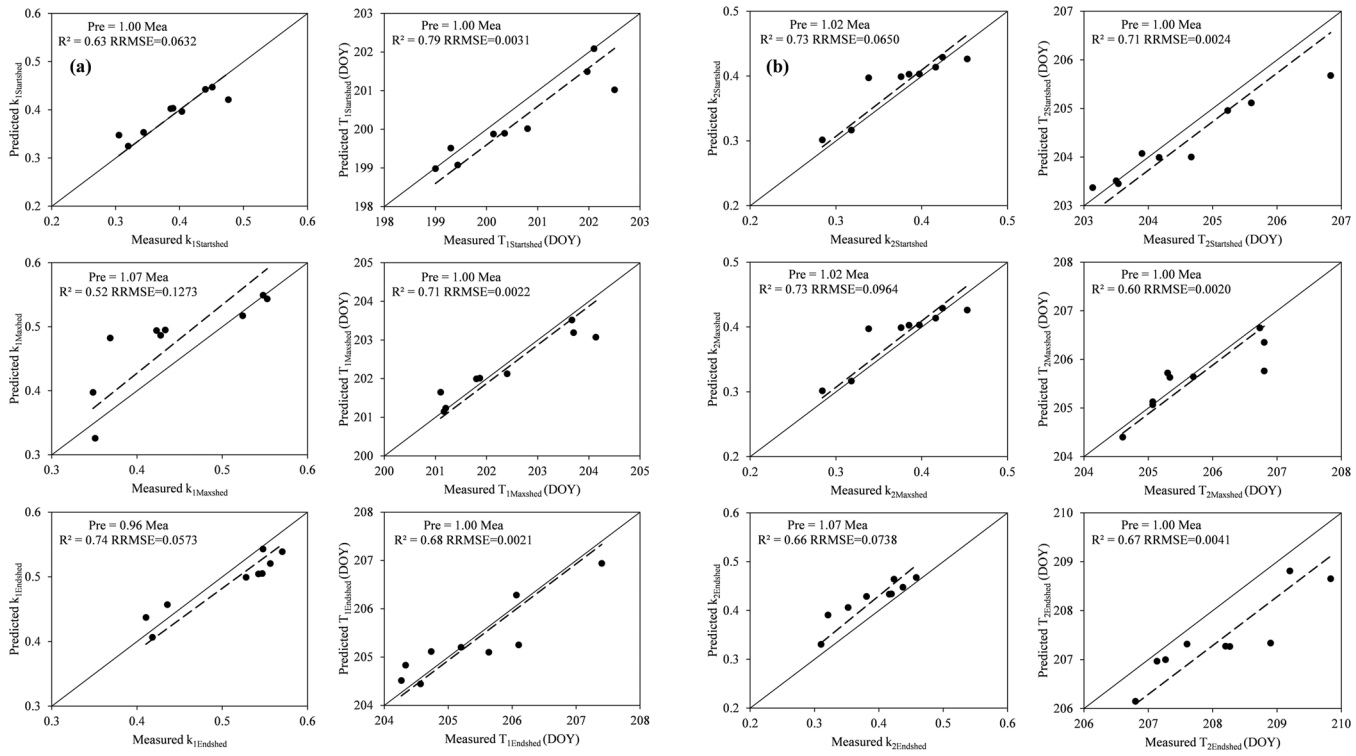

Fig. 4. Comparison between the measured flowering characteristics (Mea) of 2015 and the predicted (Pre) value with the parameters calibrated by 7 irrigation treatments of 2014. (a) Startshed, Maxshed and Endshed rate and time of the first batch of male population; (b) Startshed, Maxshed and Endshed rate and time of the second batch of male population. R^2, the coefficient of determination; RRMSE, the relative root mean square error.

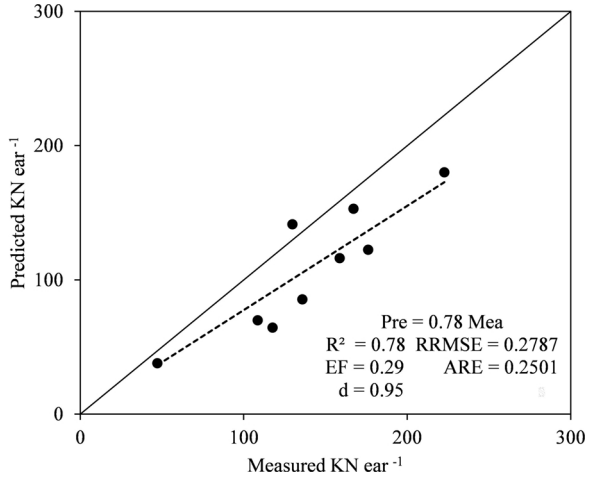

Fig. 5. Comparison between the measured kernel number ear^{-1} (Mea) of 2015 and the predicted (Pre) value with the parameters calibrated by 7 irrigation treatments of 2014. R^2, the coefficient of determination; RRMSE, the relative root mean square error.

3. Results and discussion

3.1. Flowering Model revising and Calibration of pollen density threshold

Kernel number simulated by the original Flowering Model was much higher than the measured value in all the water treatments of 2014 (Fig. 1a) with the regression coefficient (b) of 2.22, the coefficient of determination (R^2) of 0.37 and the relative root mean square error (RRMSE) of 1.2845.

The original Flowering Model assumed that 96% of pollinated silks develop into kernels. But, if water deficit happens some of the fertilized ovaries will abort and can't develop into kernels. Therefore, the original Flowering Model isn't suitable for this circumstance. The SC indicates the ability of female flowers which have received viable pollen to set kernels. When water deficit occurred at the vegetative and flowering stages, the low water potential of silk and the reduction of assimilate supply caused SC decrease (Wang et al., 2017). Therefore, when simulating kernel numbers under different water regimes using Flowering Model, the SC needs to be considered. However, the kernel number simulated by the revised Flowering Model was also higher than the measured value with a b of 1.52, a R^2 of 0.89 and a RRMSE of 0.5628 for all the treatments of 2014 (Fig. 1b).

The decrease of pollen viability may lead to an increase in the PD_{min} and a decrease in the kernel number. Thus, large errors could be expected in the simulation of the kernel number in maize used for seed production under different water conditions, as the PD_{min} was determined without quantitative pollen viability when the Flowering Model was developed (Bassetti and Wesgate, 1994; Lizaso et al., 2003). The PD_{min} therefore needed to be calibrated to make it suitable for the current study in which the average pollen viability during 0900～1000 was 0.41 (Wang et al., 2017). After incorporating the SC into the Flowering Model, the PD_{min} was calibrated as 285 grains cm^{-2} d^{-1} based on 7 treatments carried out in 2014 following the method of least squares between the measured and simulated kernel numbers. The kernel number of maize inbreds for hybrid seed production under different water conditions in 2014 were well simulated by the revised Flowering Model when the PD_{min} was calibrated, with a b of 0.98, a R^2 of 0.82 and a RRMSE of 0.1636 (Fig. 1c).

Bassetti and Wesgate (1994) carried out the experiment at Morris, Minnesota, USA (45°35′N, 95°54′W, altitude 345 m) in 1990. From 10 July to 10 August when the temperature was highest and maize was at the flowering stage, the highest maximum temperature was 32.8℃, and there was only one day when temperature was higher than 32℃. In our experiments, from 10 July to 10 August when the temperature was highest and maize was at the flowering stage, the highest maximum temperature was 36.2℃ and 35.3℃, there were 11 and 13 days when

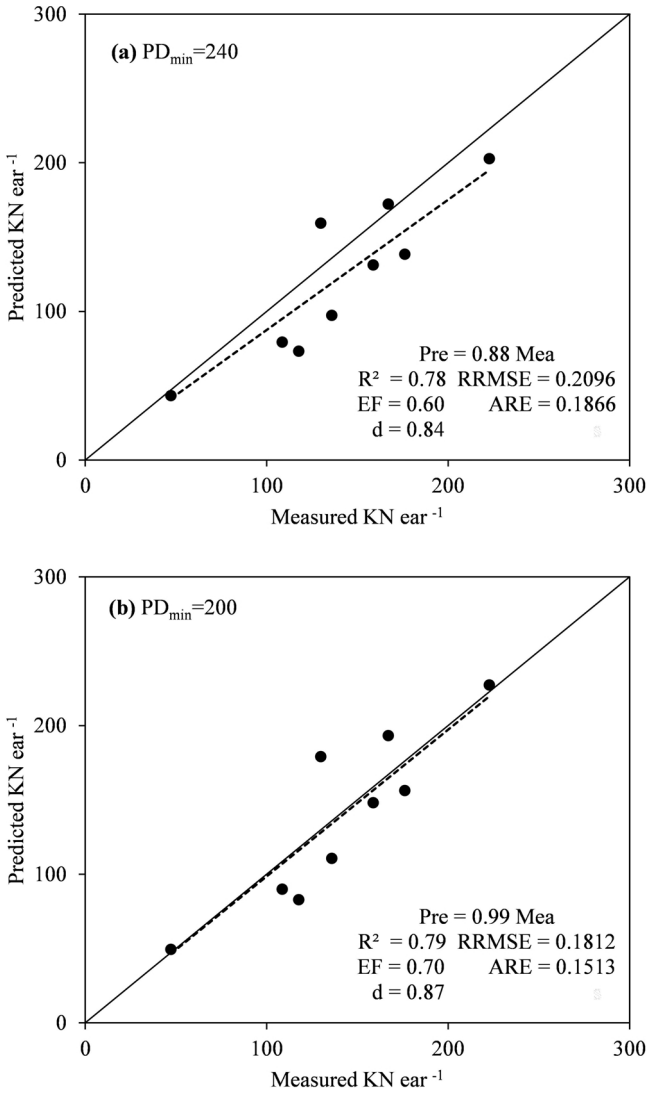

Fig. 6. Comparison between the measured kernel number ear^{-1} (Mea) of 2015 and the predicted (Pre) value with the parameters calibrated by 7 irrigation treatments of 2014. (a) PD_{min} was set as 240 grains cm^{-2} d^{-1}; (b) PD_{min} was set as 200 grains cm^{-2} d^{-1}. R^2, the coefficient of determination; RRMSE, the relative root mean square error.

temperature was higher than 32 °C in 2014 and 2015 respectively (Fig. 2). Herrero and Johnson (1980) indicated that prolonged exposure to temperatures above 32 °C can reduce pollen germination of many genotypes to levels near zero. Even though the rainfall from 10 July to 10 August was higher at Wuwei in 2014 and 2015 than at Morris in 1990, there was no rain when temperature was higher than 30 °C resulting in a higher vapor pressure deficit. Therefore, the pollen viability of our research was lower than that in Bassetti and Wesgate (1994). Differences in maize varieties also lead to differences in pollen viability (Fonseca and Westgate, 2005; Herrero and Johnson, 1981). Moreover, the sterile pollen grains occupying the position on silks might make the fertile pollen grains hard to fall on silks. Thus, the PD_{min} needed to achieve 96% kernel set was higher in our research than in Bassetti and Wesgate (1994).

3.2. Water sensitivity index of flowering characteristics

The water sensitivity indexes of k_f, T_f, k_e, SN_X, SC and TPD at the vegetative and flowering stages for the Jensen model, Minhas model, Blank model and Stewart model (Eq. 8–11) calibrated by 7 irrigation treatments of 2014 are given in Table 3, with R^2 of 0.70 ~ 0.99 and RRMSE of 0.0014 ~ 0.1188. The R^2 of Jensen model and Stewart model was always at a relative high level, and the RRMSE was always at a relative low level. The water sensitivity indexes of Startshed, Maxshed and Endshed rate and time of the two batches of male population (k_{jg} and T_{jg}) calibrated by 7 irrigation treatments of 2014 are given in Table 4, with R^2 of 0.57 ~ 0.96 and RRMSE of 0.0015 ~ 0.0504.

The field experimental data obtained in 2015 was used to validate the water sensitivity indexes calibrated by the field data of 2014. Fig. 3 shows the comparisons between the measured k_f (a), T_f (b), k_e (c), SN_X (d), SC (e) and TPD (f) and the predicted values obtained from Jensen, Minhas, Blank and Stewart models. For Jensen model, b was 0.95 ~ 1.03, R^2 was 0.50 ~ 0.85, RRMSE was 0.0047 ~ 0.1100. For Minhas model, b was 0.92 ~ 1.01, R^2 was 0.21 ~ 0.81, RRMSE was 0.0095 ~ 0.3432. For Blank model, b was 0.99 ~ 1.07, R^2 was 0.15 ~ 0.79, RRMSE was 0.0067 ~ 0.1297. For Stewart model, b was 0.98 ~ 1.04, R^2 was 0.22 ~ 0.82, RRMSE was 0.0095 ~ 0.4250. The performance of Jensen model in predicting flowering characteristics (k_f, T_f, k_e, SN_X, SC and TPD) was better than other three models. The predicted k_f, T_f, k_e, SN_X, SC and TPD were close to the measured ones and most of the variation of the measured values was explained by Jensen model. Therefore, Jensen model can be used for simulating the effect of water deficit at the vegetative and flowering stages on flowering characteristics (k_f, T_f, k_e, SN_X, SC and TPD) and the water sensitivity index derived from Jensen model with the experiment data of 2014 was used for predicting the kernel number of 2015.

Fig. 4 shows the comparisons between the measured k_{jg} and T_{jg} and the predicted values with b of 1.00 ~ 1.07, R^2 of 0.52 ~ 0.79 and RRMSE of 0.0020 ~ 0.1273. The predicted values were close to the measured ones and most of the variation of the measured values was explained by the model. Therefore, Eq. (12) can be used for simulating the effect of water deficit at vegetative stage on flowering characteristics (k_{jg} and T_{jg}) and the water sensitivity index derived from Eq. (12) with the experiment data of 2014 was used for predicting the kernel number of 2015.

3.3. Water-Flowering Model validation

The PD_{min} was calibrated as 285 grains cm^{-2} d^{-1} by the experiment data of 2014 and the water sensitivity indexes of flowering characteristics in Jensen model and Eq. (12) were also calibrated by the experiment data of 2014. With these calibrated parameters and the measured evapotranspiration, the kernel number of different water treatments in 2015 were predicted by Water-Flowering Model. Comparison between the measured kernel number of different irrigation treatments in 2015 and the values predicted by Water-Flowering Model was shown in Fig. 5, with a b of 0.78, R^2 of 0.78, RRMSE of 0.2787, EF of 0.29, ARE of 0.2501 and d of 0.84. The result was just satisfied and the proposed Water-Flowering Model can be adapted readily to accommodate a range of water conditions altering flower development and function. But the model underestimated kernel number in most irrigation treatments of 2015.

The main reason for the underestimated kernel number may be the unsuitable PD_{min}. Then we decreased the PD_{min} to predict kernel numbers of 2015 and found that when PD_{min} = 240 grains cm^{-2} d^{-1} the performance of the model was better with b of 0.88, R^2 of 0.78, RRMSE of 0.2096, EF of 0.60, ARE of 0.1866 and d of 0.90 (Fig. 6a). When PD_{min} = 200 grains cm^{-2} d^{-1} the performance of the model was much better with b of 0.99, R^2 of 0.79, RRMSE of 0.1812, EF of 0.70, ARE of 0.1513 and d of 0.93 (Fig. 6b).

The value of 0.41 was the pollen viability during 0900 ~ 1000 of one day. Pollen viability was not affected by water deficit, but it would decrease with increasing temperature (Schoper et al., 1986) and decreasing humidity (Fonseca and Westgate, 2005). Therefore, pollen viability might be lower during midday and afternoon, and would change with different meteorological conditions in other days. The

PD_{min} we got from calibration was an average value during flowering stage. Therefore, some efforts should be taken in the future to study the relationship between the PD_{min} and the meteorological condition.

4. Conclusion

When simulate kernel number under different water regimes in hybrid maize seed production, the SC should be incorporated into the Flowering Model. The k_f, T_f, k_e, SN_X, SC and TPD can be predicted by the evapotranspiration of vegetative and flowering stages using Jensen model, and the k_{jg} and T_{jg} can be predicted by evapotranspiration of vegetative stage. Combining the above models, the Water-Flowering Model was proposed. To some extent, it was validated. But it is important to emphasize that the PD_{min} was based on the meteorological condition and the quantitative relationship between PD_{min} and meteorological factors should be developed to accurately predict kernel number using Water-Flowering Model in hybrid maize seed production.

Acknowledgements

We are grateful for financial support from the National Natural Science Fundation of China (91425302, 51621061), the Ministry of Agriculture of China Special Fund for Agro-Scientific Research in the Public Interest (201503125), and the Ministry of Education of China 111 Project (B14002).

References

Alqudah, A.M., Samarah, N.H., Mullen, R.E., 2011. Drought stress effect on crop pollination, seed set, yield and quality. In: Lichtfouse, E. (Ed.), Alternative Farming Systems, Biotechnology, Drought Stress and Ecological Fertilization. Springer, 233 Spring Street, New York, NY 10013, pp. 193–213.

Bassetti, P., Wesgate, M.E., 1994. Floral asynchrony and kernel set in maize quantified by image analysis. Agron. J. 86, 699–703.

Bassetti, P., Westgate, M.E., 1993. Water deficit affects receptivity of maize silks. Crop Sci. 33, 279–282.

Blank, H.G., 1975. Optimal Irrigation Decisions with Limited Water. Colorado State University, Fort Collins, CO.

Çakir, R., 2004. Effect of water stress at different development stages on vegetative and reproductive growth of corn. Field Crops Res. 89, 1–16.

Chen, J.L., Kang, S.Z., Du, T.S., Guo, P., Qiu, R.J., Chen, R.Q., Gu, F., 2014. Modeling relations of tomato yield and fruit quality with water deficit at different growth stages under greenhouse condition. Agric. Water Manage. 146, 131–148.

Coucheney, E., Buis, S., Launay, M., Constantin, J., Mary, B., de Cortázar-Atauri, I.G., Ripoche, D., Beaudoin, N., Ruget, F., Andrianarisoa, K.S., 2015. Accuracy, robustness and behavior of the STICS soil–crop model for plant, water and nitrogen outputs: evaluation over a wide range of agro-environmental conditions in France. Environ. Model. Softw. 64, 177–190.

Dudley, N.J., Howell, D.T., Musgrave, W.F., 1971. Optimal intraseasonal irrigation water allocation. Water Resour. Res. 7, 770–788.

Fonseca, A.E., Westgate, M.E., 2005. Relationship between desiccation and viability of maize pollen. Field Crops Res. 94, 114–125.

Fonseca, A.E., Lizaso, J.I., Westgate, M.E., Grass, L., Dornbos, D.L., 2004. Simulating potential kernel production in maize hybrid seed fields. Crop Sci. 44, 1696–1709.

Fuad-Hassan, A., Tardieu, F., Turc, O., 2008. Drought-induced changes in anthesis-silking interval are related to silk expansion: a spatio-temporal growth analysis in maize plants subjected to soil water deficit. Plant Cell Environ. 31, 1349–1360.

Herrero, M.P., Johnson, R.R., 1980. High temperature stress and pollen viability of maize. Crop Sci. 20, 796–800.

Herrero, M.P., Johnson, R.R., 1981. Drought stress and its effects on maize reproductive systems. Crop Sci. 21, 105–110.

Horner, H.T., Palmer, R.G., 1995. Mechanisms of genic male sterility. Crop Sci. 35, 1527–1535.

Jensen, M.E., 1968. Water Consumption by Agricultural Plants. Academic Press, New York.

Kang, S.Z., Shi, P., Pan, Y.H., Liang, Z.S., Hu, X.T., Zhang, J., 2000. Soil water distribution, uniformity and water-use efficiency under alternate furrow irrigation in arid areas. Irrig. Sci. 19, 181–190.

Kang, S.Z., Hao, X.M., Du, T.S., Tong, L., Su, X.L., Lu, H.N., Li, X.L., Huo, Z.L., Li, S.E., Ding, R.S., 2017. Improving agricultural water productivity to ensure food security in China under changing environment: from research to practice. Agric. Water Manage. 179, 5–17.

Kiesselbach, T.A., 1980. The Structure and Reproduction of Corn. University of Nebraska Press, Lincoln.

Lizaso, J.I., Westgate, M.E., Batchelor, W.D., Fonseca, A., 2003. Predicting potential kernel set in maize from simple flowering characteristics. Crop Sci. 43, 892–903.

Minhas, B.S., Parikh, K.S., Srinivasan, T.N., 1974. Toward the structure of a production function for wheat yields with dated inputs of irrigation water. Water Resour. Res. 10, 383–393.

Schoper, J.B., Lambert, R.J., Vasilas, B.L., 1986. Maize pollen viability and ear receptivity under water and high temperature stress. Crop Sci. 26, 1029–1033.

Stewart, J.I., Misra, R.D., Pruitt, W.O., Hagan, R.M., 1975. Irrigating corn and grain sorghum with a deficient water supply. Trans. ASAE 18, 270–280.

Wang, J.T., Tong, L., Kang, S.Z., Li, F.S., Zhang, X.T., Ding, R.S., Du, T.S., Li, S.E., 2017. Flowering characteristics and yield of maize inbreds grown for hybrid seed production under deficit irrigation. Crop Sci. 57, 1–13.

Westgate, M.E., Boyer, J.S., 1986a. Reproduction at low silk and pollen water potentials in maize. Crop Sci. 26, 951–956.

Westgate, M.E., Boyer, J.S., 1986b. Silk and pollen water potentials in maize. Crop Sci. 26, 947–951.

Wilson, J., Allison, J., 1978. Effects of water stress on the growth of maize (Zea mays L.). Rhodesian J. Agri. Res. 16, 175–192.

Yang, J.M., Yang, J.Y., Liu, S., Hoogenboom, G., 2014. An evaluation of the statistical methods for testing the performance of crop models with observed data. Agric. Syst. 127, 81–89.